

2 Engineering Functionalized Graphene-based Films at the Sub-Micron- and Nanometer-Length Scales

This chapter presents work inspired by discussions with Benjamin Hatton from the laboratory of Prof. Johanna Aizenberg at Harvard University and Michael Pope at Princeton University.

2.1 Introduction

The microstructure and nanostructure of an FGS-based EDLC electrode will ultimately govern its performance. In this respect, understanding how nanomaterials can be assembled is critical to designing EDLCs with tailored energy and power densities. This chapter explores two approaches to design FGS-based electrodes at two different length scales: the sub-micron (0.01-1 μm) and nanometer (1-10 nm) scales, shown in Figure 2.1. Though engineering the porosity at the sub-micron scale is not the bottleneck impeding the design of high energy density EDLCs, as will be discussed, porosity at this length scale holds promise in developing hierarchically porous structures with improved rate performance.¹⁻⁴ More importantly, my initial work in developing porous FGS-based structures on the sub-micron length scale revealed the scientific and technological problem upon which the foundation of this thesis was constructed. As such, the work in this chapter is presented in the order in which it was performed to not only give broader context to the complexity of “porosity” in graphene-based devices, but to reflect the general progression of my work

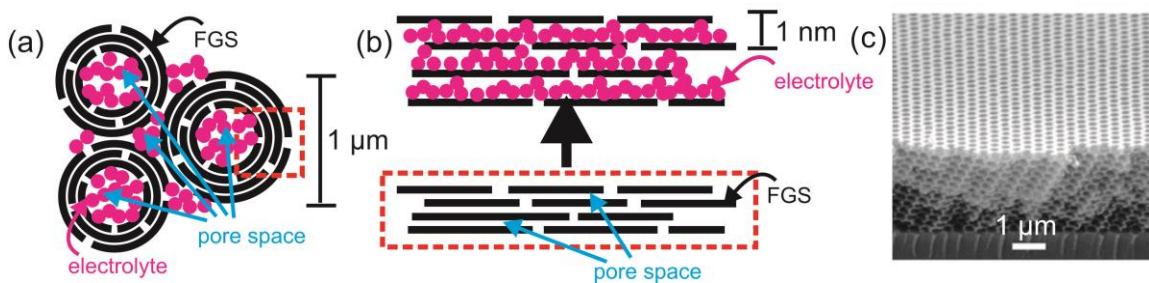


Figure 2.1: Porosity of FGS-based films. (a) Cartoon highlighting inter-aggregate porosity formed between densely packed FGSs and (b) the intra-particle porosity between the individual FGSs. High energy density EDLCs will require the clever engineering of the intra-particle porosity, while high power density devices will require larger, inter-particle porosity featured in (a). (c) Example of an inverse opal composed of titania after the opal template has been removed, reproduced by Hatton *et al.* *PNAS*, 2010.

and the scientific research conducted in the field of graphene-based electrodes during my graduate studies.

The first processing strategy relies on a technique used to develop inverse opals, a type of photonic crystal typically constructed from the templating of a metal oxide onto an organic-based colloidal crystal. An example of a titania-based inverse opal is shown in Figure 2.1(c). Hatton and his colleagues at Harvard University developed a facile route to co-assemble colloidal particles and a solution of a small-molecule silica precursor into ordered, crack-free opal structures.⁵ Michael Pope and I proposed to substitute FGS for the silica precursor, in an attempt to create three-dimensional macrostructures of FGSs with interconnected porosity, structures which held promise not only for EDLCs, but also for lithium-ion batteries, dye-sensitized solar cells, sensors and adaptive materials.

These efforts sparked questions and subsequent ideas about not only controlling the sub-micron scale porosity, but also the “porosity” between individual FGSs at the nanometer length scale as the dense packing of active material and electrolyte is currently hypothesized to produce the EDLC electrode with the highest energy density. The second

processing strategy, inspired by the co-assembly concept of prior inverse opals work, consisted of consolidating functionalized graphene directly with high-voltage room temperature ionic liquid (RTIL) electrolytes. By controlling the RTIL content, we investigated whether a simple processing procedure, such as the mechanical mixing of the two components, could produce electrodes with high gravimetric capacitance. In effect, these efforts were beginning to use the electrolyte as a structural component in the construction of the EDLC electrode.

2.2 Experimental Methods

The following sections contain experimental information pertinent to the work discussed in this Chapter.

2.2.1 Materials

2.2.1.1 Preparation of GO and graphene oxide

GO was prepared using the “improved Hummers method” detailed by Marcano *et al.* and reproduced here with slight modifications.⁶ Briefly, 360 mL of concentrated sulfuric acid (98%) and 40 mL of concentrated phosphoric acid (85%) were added to a 1 L beaker placed in an oil bath. The acids were mixed with a PTFE stir bar. Next, 3.0 g graphite (Asbury Grade 3061) was added to the mixture followed by 18.0 g of potassium permanganate. Initially, the reaction mixture is a deep green color. The temperature of the reaction mixture was maintained between 40 and 45°C, which is 5-10°C lower than that suggested by Marcano *et al.* and was stirred for 16 h, (a time 33% longer than that recommended by Marcano *et al.*) The reaction was cooled by pouring the reaction mixture

into a 2 L beaker filled with 400 g of ice. At this stage the reaction mixture was a deep purple color. Aliquots of 3 mL hydrogen peroxide (35 wt%) were added to the reaction mixture until it turned a bright yellow color (about 3-4 aliquots). A “perfect” processing occurs when all of the flecks in the reaction mixture are completely white, *i.e.*, when no grey/black flecks, which are indicative of un-oxidized graphite are observed. At the end of the reaction, the solid product is referred to as GO.

The reaction mixture was partitioned between two 500 mL centrifuge tubes and centrifuged at 3000 RPM (2000 *g*-force, IEC Centrifuge with 269 swinging bucket rotor) for 45 min. The supernatant was decanted and the GO pellet was re-suspended in 300 mL of water, mechanically stirred and centrifuged again; ultrasonication was not used. This washing procedure was repeated with 35 wt% hydrochloric acid (3x) and finally with anhydrous ethanol (3x). After the final ethanol wash, the GO was stored in ethanol in an Erlenmeyer flask until use or powder processing (detailed in the next Section). Mechanical stirring of the graphene oxide-ethanol mixture resulted in exfoliation of individual graphene oxide sheets. Therefore, the suspension likely contains a majority of graphene

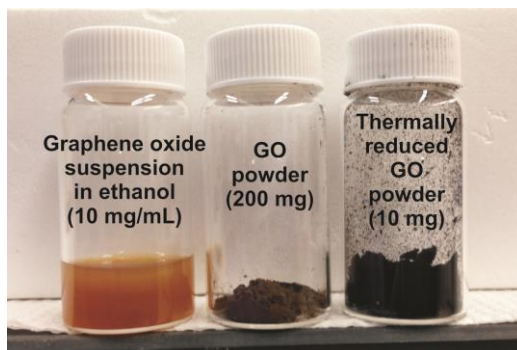


Figure 2.2: Graphene oxide, GO and thermally reduced GO. From left to right: graphene oxide-ethanol suspension, GO powder and thermally reduced GO powder produced via thermal exfoliation and reduction of GO powder (1100°C for 60 s).

oxide single sheets and aggregates and a trace amount of GO. The concentration of the graphene oxide suspension at this stage is typically between 10-20 mg/mL. A sample of the suspension is shown in Figure 2.2.

The ethanol in the graphene oxide-ethanol can be easily exchanged with other alcohols, if desired. This is achieved through successive centrifugations, in which the pellet of the graphene oxide-ethanol suspension is washed and re-suspended via mechanical agitation in the desired alcohol. The ethanol can also be exchanged with water, though at comparable concentrations (10-20 mg/mL) we find that the graphene oxide suspension forms a gel.

2.2.1.2 GO Powder

The graphene oxide-ethanol suspension can be used as-is or the material can be further processed into a “dry” powder by spray drying.⁷ To process the material into a powder, the graphene oxide-ethanol suspension was again centrifuged, and the GO pellet was re-suspended in water to achieve a suspension which is approximately 2 mg/mL. At this concentration and in an aqueous environment, the suspension was highly viscous and gel-like. To prevent clumping of the material, the water was added slowly to the GO under constant stirring and was left stirring for 24-48 hours prior to spray-drying. The suspension was spray dried (Niro portable spray dryer, Niro, Inc.) with an inlet air temperature near 300°C and outlet air temperature below 110°C. The powder was collected and stored in a scintillation vial. A sample of the spray-dried material is shown in Figure 2.2.

2.2.1.3 Preparation of Thermally Reduced GO and FGSs

Thermal exfoliation and reduction of GO was performed in a tube furnace according to a procedure developed in our group.⁷⁻⁸ Typically, 100 mg of the as-prepared GO powder

was placed in the bottom of a fused quartz tube. The powder was dried overnight under nitrogen flow in an attempt to remove adsorbed water which may have remained on the material. The tube was evacuated and filled with ultra-pure argon gas (99.9995%) three times to ensure that the atmosphere in the tube was oxygen-free. The tube was then held under vacuum and passed into the hot zone of a Lindburg furnace which was pre-heated to a desired temperature (typically between 300°C and 1100°C) for 30 to 60 s. The tubes were removed from the furnace and allowed to cool on graphite-coated bricks as the tube can be red-hot especially at the higher temperatures. The powder was vacuumed out of the tube, collected and stored in aluminum foil to shield the low-density material from static charge. Figure 2.2 shows a sample of this low-density material. The carbon to oxygen ratio (C/O) of the material was measured via energy dispersive X-Ray spectroscopy (Section 2.2.2.3) is typically used as a measure of the degree of reduction (with GO having C/O ~2). The C/O of thermally reduced GO prepared at 1100°C for 60 s is approximately 20.

The thermally reduced GO features a vermiculite structure composed of expanded, yet stacked domains of the original GO particle. FGSs are produced by suspending thermally reduced GO in an appropriate solvent and ultrasonically to exfoliate the vermiculite structure into individual sheets; these sheets are referred to as FGSs.

2.2.1.4 Synthesis of Polystyrene Spheres

Polystyrene spheres were prepared via an aqueous surfactant-free emulsion polymerization detailed in the literature.⁹ After synthesis, the polystyrene spheres were extensively washed by dialyzing against Picopure® water (18 MΩ from tap) for two weeks. Approximately 20 volume exchanges were made with the ratio of the volume of the

reservoir to the volume of the dialysate being 100. The spheres were characterized via SEM and dynamic light scattering. The experimental protocol was tailored to produce spheres of two different sizes: 300 and 700 nm. The larger spheres had a polydispersity index of 0.3. The concentration of the stock suspension of polystyrene spheres was measured to be 80 mg/mL.

2.2.1.5 Evaporation-Induced Colloidal Assembly

The procedure used to make the inverse opal structures was adapted from Hatton *et al.* and encompasses an evaporation-induced co-assembly of colloidal spheres (which serve as the opal template) and an additional component to fill the void space between the spheres.⁵ Removal of the spheres via heat treatment results in a structure described as an “inverse opal,” which features an array of inter-connected pore spaces. Briefly, strips of silicon wafers (1 x 4 cm) were soaked in “piranha” base (1:1:5, ammonium hydroxide:hydrogen peroxide:distilled water by volume, heated to 85°C) for 10 min. to both remove organic contaminants from the surface and also hydroxylate the wafer as a hydrophilic surface is needed for the assembly. The cleaned silicon wafer strips were placed vertically along the perimeter of a 25 mL beaker. A suspension of polystyrene spheres (4 vol%) in water was prepared from the stock suspension and bath sonicated for 20 min. to ensure the spheres were dispersed.

Two types of graphene-based suspensions were prepared. The first was an aqueous suspension of FGS (Batch 3030 provided by Vorbeck Materials, C/O of 33 measured by EDS) with triblock copolymer surfactant (ethylene oxide₁₀₀-propylene oxide₆₅-ethylene oxide₁₀₀, F-127, Pluronic), which is added to enable the dispersion of the hydrophobic

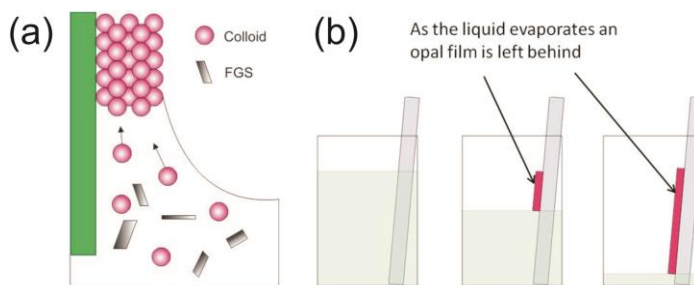


Figure 2.3: Schematic of evaporation-induced colloidal co-assembly. (a) Co-assembly of colloidal particles at the meniscus between a substrate (green) and a suspension of colloids (polystyrene spheres) and FGS. Modified from Hatton *et al. PNAS*, **2010**. (b) Schematic of film growth (pink) with evaporation of solvent against a solid substrate.

material (FGS) in water.¹⁰ Briefly, 10 mg of triblock-copolymer was dissolved in 10 mL water. 10 mg of FGS was slowly added while tip sonicating (40% amplitude, Vibra-Cell, Sonics) on ice for approximately 1 h. The prepared suspension was centrifuged at 900 g for 10 min to remove large agglomerates. Two concentrations, 0.1 and 0.45 mg/mL were prepared by further diluting this stock suspension with distilled water. Secondly, aqueous suspensions of graphene oxide were prepared by dispersing GO powder in water (1 mg/mL). These suspensions were briefly tip sonicated on ice for 10 min before use. Additionally, a hydrolyzed tetraethylorthosilicate (TEOS) precursor solution (1:1:1.5 weight ratio of TEOS:0.10 M hydrochloric acid:ethanol) was used to reproduce the silica inverse opal structures reported by Hatton *et al.* These structures serve as our control to ensure that the original procedure was being executed correctly.

Either the FGS-triblock copolymer or graphene oxide suspension (20 mL) was added to the beaker followed by 1 mL of the 4 vol% polystyrene suspension. The beaker was placed in a 65°C oven and was removed when the liquid had evaporated and a film had deposited on the silicon wafer strip, shown schematically in Figure 2.3. The composite

films on the silicon wafer strips were analyzed as-is or subjected to heat treatment to remove the polystyrene spheres (and/or triblock-copolymer) and reduce the graphene oxide to conductive FGS. The films were heated under nitrogen in a tube furnace at a 2°C/min ramp rate to 400°C with a 30 min. hold at this temperature to ensure complete polystyrene degradation.

2.2.2 Physical Characterization

2.2.2.1 Scanning Electron Microscopy

FGS-based films were visualized using scanning electron microscopy (SEM, Tescan 5130MM) under 10 or 20 kV accelerating voltage. For cross-sectional images, the samples were fixed to aluminum sample holders with a 45° incline using conductive carbon tape. Images of insulating samples were taken after sputter coating with a 2 nm thick layer of iridium.

2.2.2.2 Powder X-Ray Diffraction

To analyze the spacing between the graphene oxide sheets (referred to as the d_{0002} spacing, based on the crystallographic structure of GO), XRD spectra were recorded using a desktop diffractometer (Rigaku MiniFlex II) with a Cu K α radiation source ($\lambda = 1.54 \text{ \AA}$). Typical measurement conditions feature a sampling of 2°/min at 30 kV and 15 mA. The d_{0002} spacing of GO is fairly variable (~0.8-1 nm), but the peak is typically located near a scattering angle (2θ) of 9-11°. Larger spacing corresponds to peaks at lower scattering angles. The d_{0002} spacing is calculated from Bragg's Law as:

$$d_{0002} = \frac{\lambda n}{2 \sin \theta} \quad (2.1)$$

8. Schniepp, H. C.; Li, J.-L.; McAllister, M. J.; Sai, H.; Herrera-Alonso, M.; Adamson, D. H.; Prud'homme, R. K.; Car, R.; Saville, D. A.; Aksay, I. A. Functionalized Single Graphene Sheets Derived from Splitting Graphite Oxide. *The Journal of Physical Chemistry B*, **2006**, *110*, 8535-8539.
9. Goodwin, J. W.; Hearn, J.; Ho, C. C.; Ottewill, R. H. Studies on preparation and characterization of monodisperse polystyrene latices 3. Preparation without added surface-active agents. *Colloid Polymer Science*, **1974**, *252*, 464-471.
10. Korkut, S.; Roy-Mayhew, J. D.; Dabbs, D. M.; Milius, D. L.; Aksay, I. A. High Surface Area Tapes Produced with Functionalized Graphene. *ACS Nano*, **2011**, *5*, 5214-5222.
11. Vickery, J. L.; Patil, A. J.; Mann, S. Fabrication of Graphene-Polymer Nanocomposites With Higher-Order Three-Dimensional Architectures. *Advanced Materials*, **2009**, *21*, 2180-2184.
12. Tkalya, E.; Ghislandi, M.; Alekseev, A.; Koning, C.; Loos, J. Latex-based concept for the preparation of graphene-based polymer nanocomposites. *Journal of Materials Chemistry*, **2010**, *20*, 3035-3039.
13. Li, Y.; Wang, Z.; Yang, L.; Gu, H.; Xue, G. Efficient coating of polystyrene microspheres with graphene nanosheets. *Chemical Communications*, **2011**, *47*, 10722-10724.
14. Hong, J.; Char, K.; Kim, B.-S. Hollow Capsules of Reduced Graphene Oxide Nanosheets Assembled on a Sacrificial Colloidal Particle. *The Journal of Physical Chemistry Letters*, **2010**, *1*, 3442-3445.
15. Wang, Y.; Shi, Z.; Huang, Y.; Ma, Y.; Wang, C.; Chen, M.; Chen, Y. Supercapacitor Devices Based on Graphene Materials. *The Journal of Physical Chemistry C*, **2009**, *113*, 13103-13107.
16. Stoller, M. D.; Park, S.; Zhu, Y.; An, J.; Ruoff, R. S. Graphene-Based Ultracapacitors. *Nano Letters*, **2008**, *8*, 3498-3502.
17. Liu, C.; Yu, Z.; Neff, D.; Zhamu, A.; Jang, B. Z. Graphene-Based Supercapacitor with an Ultrahigh Energy Density. *Nano Letters*, **2010**, *10*, 4863-4868.